Photoemission from Pyrene and its Derivatives

Shojun HINO, Tomohiko HIROOKA*, and Hiroo INOKUCHI

The Institute for Solid State Physics, The University of Tokyo, Roppongi, Minato-ku, Tokyo 106

**Department of Chemistry, Faculty of Science, The University of Tokyo, Hongo, Tokyo 113*

(Received July 11, 1974)

Photoemissions from pyrene and its derivatives, 1,3,6,8-tetrachloropyrene(TClP), 1,3,6,8-tetrabromopyrene(TBrP), 1,6-dicyanopyrene(CDNP), 1,3,6,8-tetracyanopyrene(TCNP), and 1,3,6,8-tetranitropyrene (TNO_2P), were measured. Their photoelectron energy distribution curves(EDCs) were thus obtained; the peaks or shoulder appearing on the EDCs correspond to the ionization potentials of the pyrene molecule. Further, the spectral dependences of their quantum yields(SDQYs) were measured. The ionization potentials obtained from their threshold values were 5.8 eV(pyrene), 6.3 eV(TClP), 6.0 eV (TBrP), 6.3 eV(DCNP), 6.2 eV(TCNP), and 6.6 eV(TNO_2P).

Changes in photoelectron spectra have often been investigated by introducing some functional groups into the π-electron conjugated system, mostly benzene[1]; these photoelectron spectroscopic studies have been carried out in the gaseous state, but not in the solid state. However, as the material property of the solid state is our great concern, the photoemission will give us useful information on the materials in the solid state. As is well known, the photoemission from a solid material consists of three steps:

1) optical excitation process in the solid,
2) transport process in the solid, and
3) escape process from the surface

As the photoemission is a mixed phenomenon of such processes, the information obtained does not always reflect the electronic states of the materials.

The photoemission from organic molecular crystals has been measured by several workers.[2-5] Schechtman and Spicer[6] used Spicer's **k**-independent indirect-transition model[7] (disregarding photoelectron scattering in the bulk and at the surface) and succeeded in determining the energy structures of phthalocyanine and protoporphyrin. Applying a band theory to organic crystals, and also assuming that the state density of the conduction band is constant in molecular crystals, Spicer's model is effective in these materials.[8]

In this paper, we wish to present the photoelectron energy distribution curves and the spectral dependences of the quantum yields of pyrene and its derivatives.

Experimental

Samples. The samples used in this work are pyrene, 1,3,6,8- tetrachloropyrene (TClP), 1,3,6,8- tetrabromopyrene (TBrP), 1,3,6,8- tetracyanopyrene(TCNP), 1,6- dicyanopyrene(DCNP), and 1,3,6,8-tetranitropyrene(TNO_2P). The pyrene derivatives were prepared by Iwashima,[9] as has already been reported.[10]

In order to prepare the specimens for the photoemission measurement, pyrene and its derivatives were deposited onto a small copper disk (12 mm in diameter) by the sublimation method. The deposition was carried out *in vacuo* better than 10^{-5} Torr. However, the vapour pressure of pyrene was too high to deposit in such a vacuum, therefore, we were obliged to make the specimen on the cooled copper disk in a low vacuum ($\sim 10^{-4}$ Torr).

Measurements. The photoemission was measured with a half-meter Seya-Namioka-type vacuum ultraviolet monochromator. The details of the equipment attached to the monochromator were reported previously.[4] The collector of the photocell was a spherical glass one; the inside was coated with colloidal graphite, "Aquadag."

The energy distribution curves(EDCs) were obtained by recording the derivative of the photoelectron current, with respect to the retarding potential, V. Differentiation was performed by superimposing a small sinusoidal potential, ΔV (200 mV p-p, 4 Hz), upon V; the details of this have also been reported already.[5]

The quantum yield, Y, is the ratio between the number of the photoemitted electrons and the incident photons. When the quantum yield was measured, an accelerating potential was applied between the emitter and the collector enough to collect all the electrons emitted. The spectral response of the quantum yield was observed at intervals of 1 nm.

Results and Discussion

Energy Distribution Curves. Figures 1—6 are the EDCs of pyrene and its derivatives plotted as functions of the retarding potential. The numerical value beside each EDC is the energy of the incident photon. As a whole, only a few structures were found in the curves, and the dominant peaks were located at about 0 eV. These peaks grew rapidly with an increase in the incident photon energy.[11] These peaks, independent of the incident photon energy, are so-called "stationary peaks."

During the operation, the retarding potential was swept from minus voltage to plus one. The potential when the peak takes off from the base line is the stopping voltage, V_0, and the potential when the peak falls down to the base line is the saturation voltage, V_s. When the EDC has a tail, V_0 and V_s were determined by approximating the edges of the EDCs by straight lines. The EDCs of pyrene derivatives, especially TClP (Fig. 2), have long tails on the V_s side: this phenomenon is, perhaps, produced by the potential drop between the sample surface and the copper disk, since a charge-up takes place. Moreover, the V_s-value changes with the energy of the incident photons. From these effects, both values, V_0 and V_s, have some ambiguities; these values are summarized in Tables 1 and 2.

When the EDCs are rewritten against the initial energy of the emitted electrons, measured with respect to the stopping potentials, V_0, this revised EDC is appropriate for organic crystals, since it is uncertain whether these materials are conductors or insulators. That is, there is no need to consider the Fermi level

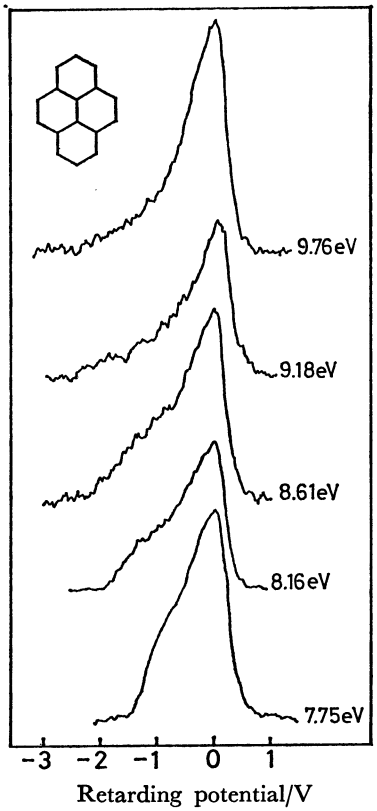

Fig. 1. Energy distribution curves of pyrene, plotted as a function of retarding potential, V, in arbitrary unit. Numerical values beside each curves (7.75 eV, 8.16 eV, 8.61 eV, 9.18 eV and 9.76 eV) are the energies of incident photon.

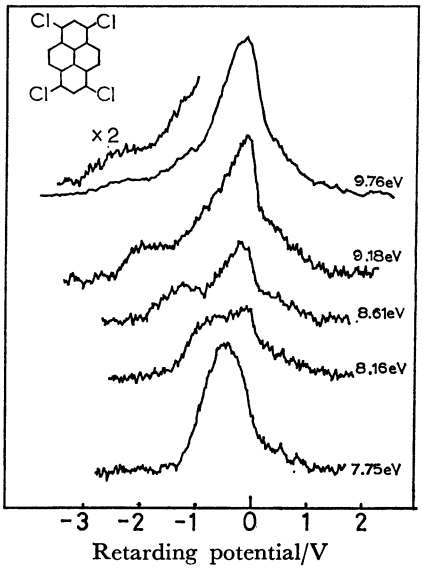

Fig. 2. Energy distribution curves of TClP. (The experimental condition is the same as Fig. 1)

in plotting.[12] Adding the threshold energy to the energy value of each peak or shoulder in EDC, which is independent of the incident photon energy in the revised plot,[13] we can find the positions of the valence bands from the vacuum levels.

In Table 3, as the peak or shoulder positions, the

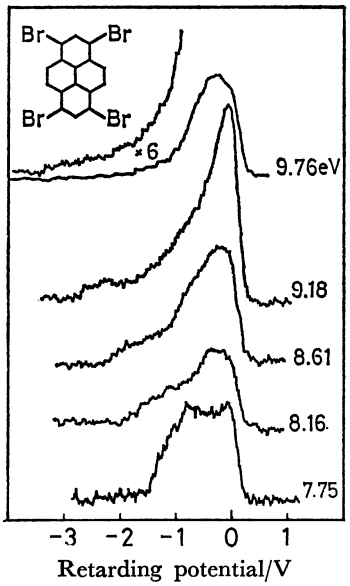

Fig. 3. Energy distribution curves of TBrP.

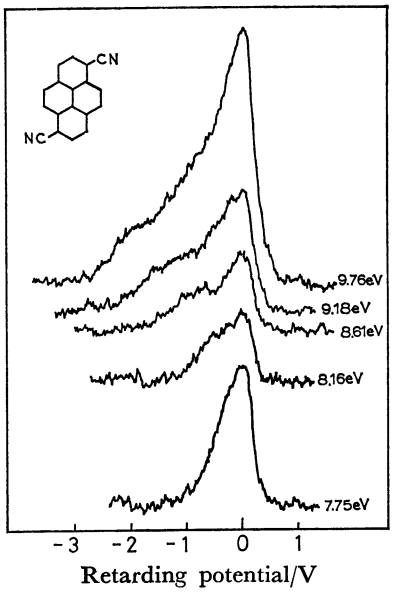

Fig. 4. Energy distribution cruves of DCNP.

energies of the optical state densities of the valence bands are listed, and the ionization potentials of pyrene in the gas phase obtained by Boschi and Schmidt[14] are also quoted. Moreover, the energy differences between the first band and the other bands are shown in Table 4.

The energy differences between the first band and the other were in good agreement with the values of Boschi's work.[14] This indicates that the locations of the first few π-bands of polycrystalline pyrene and its derivatives are similar to those of the pyrene free molecule. However, there are large differences in the shapes of their EDCs. This shape difference can be understood by considering the following several reasons:

1) The electron-attenuation lengths differ from each other; that is, the numbers of the scattering centres (π-electrons[15]) are different.

Table 1. Stoppong potentials, V_0, obtained from EDCs in V

Incident photon energy (eV)	Samples					
	Pyrene	TClP	TBrP	DCNP	TCNP	TNO_2P
7.75	−1.49	−1.25	−1.53	−1.10	−1.05	−0.82
8.16	−1.97	−1.46	−1.98	−1.46	−1.40	−1.21
8.61	−2.30	−1.91	−2.36	−1.83	−1.80	−1.81
9.18	(−2.47)	−2.43	−2.84	−2.42	−2.36	−2.38
9.76	—	−3.09	−3.42	−2.90	(−2.50)	−2.78

The values in parentheses are vague, because the determination of the onsets of the EDCs is difficult. Experimental errors were ±0.05 *V*.

Table 2. Saturation potentials, V_s, obtained from EDCs in V

Incident photon energy (eV)	Samples					
	Pyrene	TClP	TBrP	DCNP	TCNP	TNO_2P
7.75	0.42	(0.24)	0.25	0.32	0.49	0.37
8.16	0.41	(0.30)	0.25	0.38	0.50	0.38
8.61	0.34	(0.24)	0.25	0.35	0.53	0.30
9.18	0.41	(0.28)	0.23	0.42	0.59	0.36
9.76	0.42	(0.44)	0.27	0.48	0.55	0.34
Average	0.41	(0.27)	0.25	0.39	0.53	0.35

As the EDCs of TClP have long tails in V_s side, the values in this Table are the cross points of the straight parts of the EDCs and base line. Experimental errors are in ±0.05 *V*.

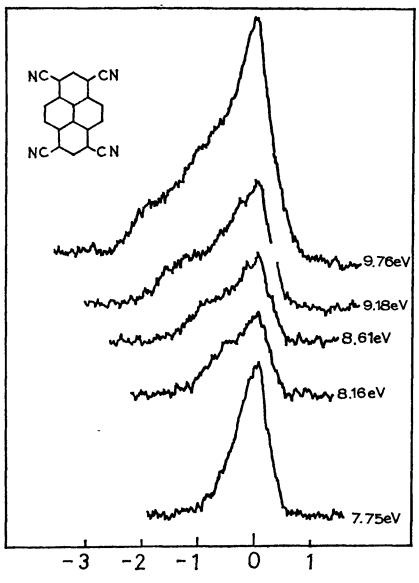

Fig. 5. Energy distribution curves of TCNP.

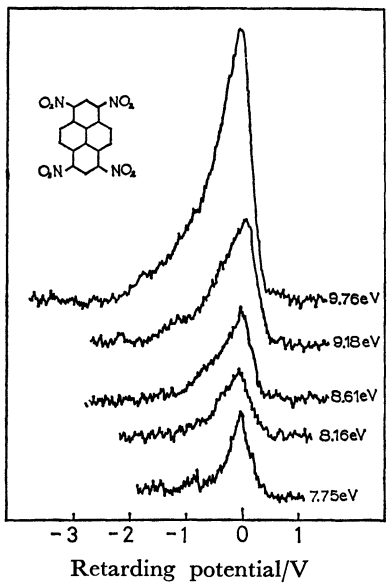

Fig. 6. Energy distribution curves of TNO_2P.

2) There are changes in crystal structures; that is, the escape probabilities of photoexcited electrons from the surface of the polycrystallines are different.

3) The surface cleanness differs, since their vapour pressures are not equal; that is, contamination of the surface by residual gas occurs.

4) Their electronic structures are changed by the functional groups; that is, the numbers of photo-excitable electrons are affected by such functional groups.

As for the first and second reasons, no data on the electron-attenuation lengths and crystal structures of these compounds are to be found, therefore, further discussion is difficult. As for the third reason, it is known that the surface of organic compounds with high vapour pressures are fairly clean in an ordinary vacuum because of their successive sublimation. This factor is useful in comparing halogen derivatives and cyano- and nitro-derivatives. From the view point of the vapour pressure, we can expect the surface of pyrene film to be clean, since its vapour pressure is the highest among these materials. On the other hand, it is also known that a contaminated surface reduces high-energy electrons to low-energy electrons; in this case, the EDCs become structureless. As the EDCs of pyrene show less structure than those of halogenized pyrenes, contamination must take place on the pyrene film. This fact is inconsistent with self-cleaning by successive sublimation. However, practically, as the spectroscopical observation was carried out in a low vacuum and with a cooled emitter, it is feasible that the surface of pyrene film is contaminated with residual gases.

In considering the fourth reason, a well-known phenomenon, mesomeric or inductive effect, is useful. Cyano- and nitro-groups are electron-withdrawing

Table 3. Peak (shoulder) positions from vacuum level in eV

	Pyrene	TClP	TBrP	DCNP	TCNP	TNO_2P	Pyrene[a)]
1st peak	(6.5_5)	6.1_5	6.7_5	(7.3_0)	(7.2_0)	7.5_0	7.41
2nd peak	(7.3_5)	(6.8_5)	(7.6_5)	(8.3_0)	(8.0_5)	(8.5_5)	8.26
3rd peak	—	(7.4_0)	(8.3_0)	—	—	—	9.00

The values in parentheses are shoulder positions. a) Ionization potentials in gas phase in Ref. 14.

Table 4. The energy differences between the first peak and the others in eV

	Pyrene	TClP	TBrP	DCNP	TCNP	TNO_2P	Pyrene[a)]
2nd	0.8_0	0.7_0	0.9_0	1.0_0	0.8_5	1.0_5	0.85
3rd	—	1.2_5	1.5_5	—	—	—	1.59

a) gas phase pyrene

functional groups (mesomeric effect). Halogen atoms have two effects: a plus mesomeric effect and a minus inductive effect. These effects increase or decrease the electron density of the pyrene-ring system; its increase or decrease may change the number of photoexcitable electrons.

Spectral Dependence of the Quantum Yield. Figure 7 shows the spectral dependences of the quantum yields (SDQYs) of pyrene and its derivatives. As may clearly be seen, pyrene has a higher photoelectron efficiency in the whole spectral region compared to those of the others. The SDQY of pyrene is about 3×10^{-2} electrons/photon at 10 eV; it gradually decreases to 7 eV, and then falls down steeply to 7×10^{-5} electrons/photon. On the other hand, the SDQYs of the substituted pyrenes show almost the same inclinations above 9 eV. However, below 9 eV those SDQYs are classified into three groups. One group (A) consists of halogen-substituted pyrenes; Group B consists of cyano-substituted pyrenes, and Group C is nitro-substituted. The SDQYs of Group A resemble those of pyrene except for the absolute value of the quantum yield; the decrease in the absolute quantum yield can be understood in terms of a deepening of the threshold energies upon the introduction of halogen atoms. The SDQYs of Groups B and C are monotonously decreasing curves, and their inclinations are steeper than those of pyrene and Group A. The quantum yield of Group C is smaller than those of Group B. These results support the fourth reason described at the EDC shape differences. Cyano- and nitro-groups induce a decrease in the cross section (the number of photoexcitable π-electrons in the pyrene-ring system) of photoemission largely by withdrawing the electrons from the pyrene-ring system. The effect of halogen atoms is not so large comparatively.

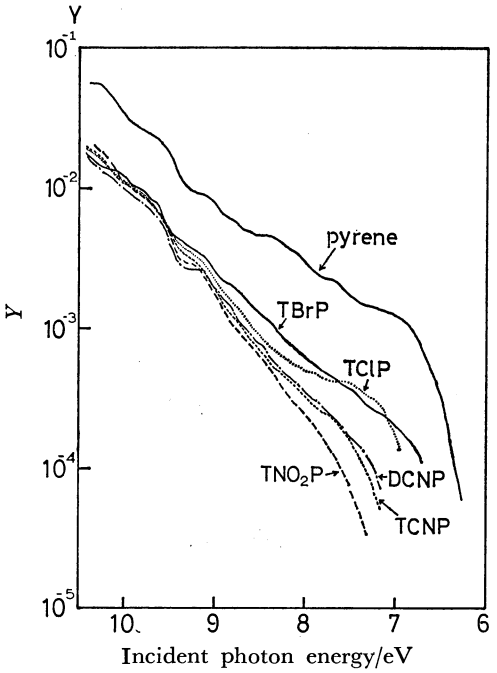

Fig. 7. Spectral dependences of quantum yields, Y, of pyrene and its derivatives, plotted as a function of incident photon energy.

Threshold Energy. To determine the ionization potential of these aromatic crystals, the threshold energy, E_{th}, is estimated by the following methods.

1) From the EDCs, with the values of V_0 and V_s, using this relations:

$$E_{th} = h\nu - V_s + V_o$$

where $h\nu$ is the incident photon energy.

2) From the SDQYs, as used by Lyons and Morris,[16] E_{th} is determined as the lowest detectable current photon energy, usually the order of $10^{-7}\sim10^{-8}$ electrons/photon as the quantum yield.

3) From the relation between the quantum yield and the incident photon energy near the threshold energy region as:

$$Y \propto (h\nu - E_{th})^3$$

In our measurments, however, there were some cases where the methods described above could not be used. The second method was especially invalid, because the lowest detectable quantum yields were in the order of $10^{-4}\sim10^{-5}$ electrons/photon, far from the order of $10^{-7}\sim10^{-8}$. The first method has some ambiguities when it is difficult to determine V_s and V_0. Moreover, as high-energy electrons often lose their energy, the determination of V_0 excited with a high-energy photon is difficult. Therefore, in this work, we adopted V_s and V_0 from the EDCs excited with 7.75 eV photons.

In the halogen-substituted pyrenes, the third method was not used, because we could not find any linear relation between $Y^{1/3}$ and $(h\nu - E_{th})$.[17] The cube-root plots of the other compounds are shown in Fig. 8.

The threshold energies obtained from the first and third methods are listed in Table 5. Batley and Lyons[18] reported the threshold energy of 1,6-diamino-

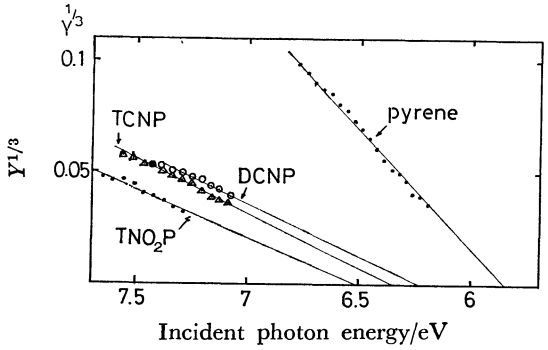

Fig. 8. Cube root of quantum yield plotted as a function of incident photon energy.

pyrene as 4.71 eV. This value is smaller than that of pyrene by more than 1 eV. As the amino group is electron-donating, the E_{th} of the amino derivative becomes small, because an electron is easily emitted from the pyrene-ring system. As for the cyano- and nitro-groups, on the other hand, the E_{th} of such substituted pyrene becomes large, because these groups are electron-withdrawing.

The authors wish to thank to Professor Satoshi Iwashima for his preparation of the materials used in this experiment.

Table 5. Threshold energies of pyrene and its derivatives in eV

	E_{th}[a)]	E_{th}[b)]
Pyrene	5.84	5.85
TClP	(6.26)	—
TBrP	5.97	—
DCNP	6.33	6.23
TCNP	6.21	6.35
TNO_2P	6.56	6.52
1,6-Diaminopyrene[c)]	4.71	

a) obtained from EDCs. b) obtained from cube root plot. c) the work of Batley and Lyons.[17)]
E_{th} of TClP has some ambiguities.
Experimental errors are in ± 0.05 eV.

References

1) For example, "Molecular Photoelectron Spectroscopy," D. W. Turner, C. Baker, A. D. Baker, and C. R. Brundle, Wiley-Interscience, London (1970).
2) A. A. Zagrubskii and F. I. Vilesov, *Fiz. Tverd. Tela*, **13**, 2300 (1971).
3) T. Hirooka, M. Kochi, J. Aihara, H. Inokuchi, and Y. Harada, This Bulletin, **42**, 1481 (1969).
4) M. Kochi, Y. Harada, T. Hirooka, and H. Inokuchi, *ibid.*, **43**, 2690 (1970).
5) T. Hirooka, K. Tanaka, K. Kuchitsu, M. Fujihira, H. Inokuchi, and Y. Harada, *Chem. Phys. Lett.*, **18**, 390 (1973).
6) B. H. Schechtman and W. E. Spicer, *ibid.*, **2**, 207 (1968).
7) W. E. Spicer, *Phys. Rev. Lett.*, **11**, 243 (1963).
8) W. E. Spicer, in F. A. Abeles (editor), "Optical Properties of Solids," North-Holland Publ. Co., Amsterdam (1972).
9) Meisei University.
10) K. Ogino, S. Iwashima, H. Inokuchi, and Y. Harada, This Bulletin, **38**, 473 (1965).
11) In Figs. 1—6, each EDC is plotted in arbitrary unit. Then, to recognize this behaviour, we must normalized each EDC with a photon intensity.
12) If Fermi level is decided by the method described in Ref. 3, obtained value for Fermi energy is changed by impurities. As impurities easily make donor and/or acceptor levels in band gap, there is an ambiguity in plot using Fermi level.
13) As the obtained EDCs were almost structureless, it is difficult to apply a Spicer's **k**-independent indirect transition model to our EDCs. It is, however, reasonable that the obtained EDCs represent the state density of the valence band, since the peak positions of our EDCs were in good agreement with orbital energies of pyrene free molecule.
14) R. Boschi and W. Schmidt, *Tetrahedron Lett.*, **25**, 2577 (1972).
15) W. Pong and J. A. Smith, *J. Appl. Phys.*, **44**, 174 (1973).
16) L. E. Lyons and G. C. Morris, *J. Chem. Soc.*, **1960**, 5192.
17) This fact should be caused purely by experimental defects. In these cases, quantum yields could be measured till about 10^{-4} electrons/photon, and the observed values were far from the regions where above relation held good.
18) M. Batley and L. E. Lyons, *Mol. Cryst.*, **3**, 357 (1968).